J|A|C|S
ARTICLES
Published on Web 06/10/2005

Blue Copper Model Complexes with Distorted Tetragonal Geometry Acting as Effective Electron-Transfer Mediators in Dye-Sensitized Solar Cells

Shigeki Hattori, Yuji Wada, Shozo Yanagida, and Shunichi Fukuzumi*

Contribution from the Department of Material and Life Science, Graduate School of Engineering, Osaka University, SORST, Japan Science and Technology Agency, Suita, Osaka 565-0871, Japan

Received February 2, 2005; E-mail: fukuzumi@ap.chem.eng.osaka-u.ac.jp

Abstract: The electron self-exchange rate constants of blue copper model complexes, [(−)-sparteine-*N*,*N*′](maleonitriledithiolato-*S*,*S*′)copper ([Cu(SP)(mmt)])$^{0/-}$, bis(2,9-dimethy-1,10-phenanthroline)copper ([Cu(dmp)$_2$]$^{2+/+}$), and bis(1,10-phenanthroline)copper ([Cu(phen)$_2$]$^{2+/+}$) have been determined from the rate constants of electron transfer from a homologous series of ferrocene derivatives to the copper(II) complexes in light of the Marcus theory of electron transfer. The resulting electron self-exchange rate constant increases in the order: [Cu(phen)$_2$]$^{2+/+}$ < [Cu(SP)(mmt)]$^{0/-}$ < [Cu(dmp)$_2$]$^{2+/+}$, in agreement with the order of the smaller structural change between the copper(II) and copper(I) complexes due to the distorted tetragonal geometry. The dye-sensitized solar cells (DSSC) were constructed using the copper complexes as redox couples to compare the photoelectrochemical responses with those using the conventional I_3^-/I^- couple. The light energy conversion efficiency (η) values under illumination of simulated solar light irradiation (100 mW/cm^2) of DSSCs using [Cu(phen)$_2$]$^{2+/+}$, [Cu(dmp)$_2$]$^{2+/+}$, and [Cu(SP)(mmt)]$^{0/-}$ were recorded as 0.1%, 1.4%, and 1.3%, respectively. The maximum η value (2.2%) was obtained for a DSSC using the [Cu(dmp)$_2$]$^{2+/+}$ redox couple under the light irradiation of 20 mW/cm^2 intensity, where a higher open-circuit voltage of the cell was attained as compared to that of the conventional I_3^-/I^- couple.

Introduction

Nanocrystalline dye-sensitized solar cells (DSSC), pioneered by Grätzel and co-workers, have attracted increasing attention as an inexpensive alternative to the conventional p−n junction solar cells.[1−5] The I_3^-/I^- redox couple has so far been employed as the best electron-transfer mediators working in DSSC.[1−5] However, the I_3^-/I^- couple has the following undesirable chemical properties.[4] First, I_3^- at high concentrations, which are required to attain the good performance, absorbs a significant amount of the visible light. Second, the low triiodide ion redox potential prevents attaining a high open-circuit voltage. A large polarization loss results from the potential mismatch between the redox couples of the sensitizers (S^+/S) and the mediator (I_3^-/I^-). Last, I_2, which is corrosive, has a substantial vapor pressure and thus would escape from the cell unless it is hermetically sealed. A number of attempts have thereby been reported to find electron-transfer mediators other than the I_3^-/I^- couple.[6−10] Although the redox potentials of some mediators, employed as rivals of I_3^-/I^-, are more positive than that of I_3^-/I^-, no significant improvement on the open-circuit potential of the cells has so far been achieved.[6−10]

In the natural electron transport systems, copper complexes, known as blue copper proteins, act as efficient electron-transfer mediators.[11−13] Plastocyanin is involved in electron transfer between Photosystems I and II in the photosynthetic chain, and azulin transfers electrons between cytochrome *c*551 and cytochrome *c* oxidase in respiratory chain.[11] Electron transfer is

(1) (a) O'Regan, B.; Grätzel, M. *Nature* **1991**, *353*, 737. (b) Grätzel, M. *Nature* **2001**, *414*, 338.
(2) (a) Hagfeldt, A.; Grätzel, M. *Chem. Rev.* **1995**, *95*, 49. (b) Hagfeldt, A.; Grätzel, M. *Acc. Chem. Res.* **2000**, *33*, 269. (c) Grätzel, M. *Pure Appl. Chem.* **2001**, *73*, 459.
(3) (a) Nazeeruddin, M. K.; Péchy, P.; Renouard, T.; Zakeeruddin, S. M.; Humphry-Baker, R.; Comte, P.; Liska, P.; Cevey, L.; Costa, E.; Shklover, V.; Spiccia, L.; Deacon, G. B.; Bignozzi, C. A.; Grätzel, M. *J. Am. Chem. Soc.* **2001**, *123*, 1613. (b) Wang, P.; Klein, C.; Humphry-Baker, R.; Zakeeruddin, S. M.; Grätzel, M. *J. Am. Chem. Soc.* **2005**, *127*, 808.
(4) Grätzel, M.; Moser, J.-E. In *Electron Transfer in Chemistry*; Balzani, V., Ed.; Wiley−VCH: Weinheim, Germany, 2001; Vol. V, pp 589−644.
(5) Hara, K.; Arakawa, H. In *Handbook of Photovoltaic Science and Engineering*; Luque, A., Hegedus, S., Eds.; John Wiley & Sons Ltd.: Chichester, UK, 2003; pp 663−700.
(6) (a) Nusbaumer, H.; Moser, J.-E.; Zakkeruddin, S. M.; Grätzel, M. *J. Phys. Chem. B* **2001**, *105*, 10461. (b) Nusbaumer, H.; Zakeeruddin, S. M.; Moser, J.-E.; Grätzel, M. *Chem.-Eur. J.* **2003**, *9*, 3756.
(7) Oskam, G.; Bergeron, B. V.; Meyer, G. J.; Searson, P. C. *J. Phys. Chem. B* **2001**, *105*, 6867.
(8) Gregg, B. A.; Pichot, F.; Ferrere, S.; Fields, C. L. *J. Phys. Chem. B* **2001**, *105*, 1422.
(9) Sapp, S. A.; Elliott, M.; Contado, C.; Caramori, S.; Bignozzi, C. A. *J. Am. Chem. Soc.* **2002**, *124*, 11215.
(10) Cameron, P. J.; Peter, L. M.; Zakeeruddin, S. M.; Grätzel, M. *Coord. Chem. Rev.* **2004**, *248*, 1447.
(11) (a) Gray, H. B.; Solomon, E. I. In *Copper Proteins*; Spiro, T. G., Ed.; Wiley: New York, 1981; pp 1−39. (b) Sykes, A. G. *Adv. Inorg. Chem.* **1991**, *107*, 377.
(12) Gross, E. L. *Photosynth. Res.* **1993**, 37, 103.
(13) (a) Groeneveld, C. M.; Canters, G. W. *J. Biol. Chem.* **1988**, *263*, 167. (b) Groeneveld, C. M.; Ouwerling, M. C.; Erkelens, C.; Canters, G. W. *J. Mol. Biol.* **1988**, *200*, 189. (c) Groeneveld, C. M.; Dahlin, S.; Reinhammar, B.; Canters, G. W. *J. Am. Chem. Soc.* **1987**, *109*, 3247. (d) Canters, G. W.; Hill, H. A. O.; Kitchen, N. A.; Adman, E. T. *J. Magn. Reson.* **1984**, *57*, 1. (e) Dahlin, S.; Reinhammar, B.; Wilson, M. T. *Biochem. J.* **1984**, *218*, 609. (f) Kyritsis, P.; Dennison, C.; Ingledew, W. J.; McFarlane, W.; Sykes, A. G. *Inorg. Chem.* **1995**, *34*, 5370.

10.1021/ja0506814 CCC: $30.25

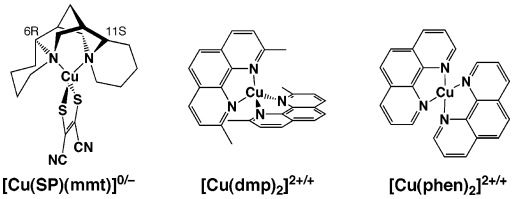

Figure 1. Structures of copper complexes used in this study.

known to proceed via transition state structures, which are intermediate between those of the reactant and product, according to the Franck−Condon principle as clarified by Marcus.[14] Thus, electron transfer does not occur until the metal center is vibrationally excited to match a geometry appropriate for that of the product complex.[14] This is accomplished by a simple adjustment in the bond lengths, but for copper such adjustment in the geometry usually requires a large energy because copper(I) and copper(II) have different preferred geometries, that is, tetrahedral and tetragonal, respectively.[15,16] In the natural system, the difference in bond lengths and geometries between copper(I) and copper(II) is cleverly minimized by the protein structure, which provides a copper site optimized for fast electron transfer.[17,18] In plastocyanin, a distorted tetragonal geometry, which is an intermediate geometry between copper(I) and copper(II), with an unusually long copper−methionine interaction is found for each oxidation state.[17,18] Plastocyanin, classified as the type I blue copper protein, compared to tetragonal copper complexes exhibits intense absorption at ca. 600 nm, distinctive electron spin resonance spectra, and unusually high redox potentials.[19,20] Considerable efforts have been devoted to the design of blue copper model complexes.[21−25] However, blue copper model complexes with favorable properties such as efficient electron transfer and high redox potentials have yet to be employed as effective electron mediators to attain the high energy conversion efficiency and high open-circuit voltages of the cells.

We report herein the use of blue copper model complexes with distorted tetragonal geometry (Figure 1) as electron-transfer mediators in DSSC in comparison with a tetragonal copper complex, $[Cu(phen)_2](CF_3SO_3)_2$ (phen = 1,10-phenanthroline), in which the four N-donor atoms are expected to be nearly coplanar. First, we employed [(−)-sparteine-*N*,*N*′](maleonitriledithiolato-*S*,*S*′)copper ([Cu(SP)(mmt)]),[25] as a blue copper model complex. Although the (−)-sparteine and the maleonitriledithiolate ligands do not accurately represent active site of the blue copper(II) proteins, the model complex closely mimics spectral and redox behaviors in the blue copper centers.[25] The intense bands in the region of 500−1000 nm are assigned to S → Cu(II) charge transfer (CT) bands.[25] A distorted tetragonal geometry is also obtained for bis(2,9-dimethy-1,10-phenanthroline)copper ($[Cu(dmp)_2](CF_3SO_3)_2$)[26−29] by introducing methyl groups in the 2,9 positions of phenanthroline ligand as a result of the steric hindrance provided by two methyl groups.[30] We have examined incident photon-to-current conversion efficiency and the photoelectrochemical responses of DSSCs containing $[Cu(SP)(mmt)]^{0/-}$, $[Cu(dmp)_2]^{2+/+}$, and $Cu(phen)_2]^{2+/+}$ in comparison with the electron-transfer properties in solution.

Experimental Section

Materials. [Cu(SP)(mmt)], $[Cu(dmp)_2](CF_3SO_3)_2$, $[Cu(dmp)_2](CF_3SO_3)$, $[Cu(phen)_2](CF_3SO_3)_2$, and $[Cu(phen)_2](CF_3SO_3)$ were prepared and characterized according to the literature.[25−29] [Cu(SP)(mmt)]Na was prepared by the reduction of [Cu(SP)(mmt)] using NaSCN aq. The Rudye, cis-dithiocyanato-*N*,*N*′-bis(4-carboxylato-4-tetrabutylammonoium-carboxylate-2,2′-bipyridine)ruthenium(II) (N719), was synthesized from *cis*-dithiocyanato-*N*,*N*′-bis(4,4′-dicarboxylate-2,2′-bipyridine)ruthenium-(II) as described in the literature.[31] Dimethylferrocene ($[Fe(C_5H_4Me)_2]$), benzoylferrocene ($[Fe(C_5H_5)(C_5H_4COOBzl)]$), and decamethylferrocene ($Fe(C_5Me_5)_2$) were purchased from Wako Pure Chemical Industries Ltd. All solvents and chemicals were of reagent grade quality, and they were purchased and used without further purification unless otherwise noted.

Electron-Transfer Kinetics of Copper Complexes. Kinetic measurements for electron transfer from ferrocene derivatives to copper(II) complexes were carried out using a UNISOKU RSP-601 stopped-flow rapid scan spectrometer in deaerated acetonitrile at 298 K. In each case, it was confirmed that the rate constants of electron transfer (k_{et}) derived from at least five independent measurements agreed within an experimental error of ±5%. Pseudo-first-order rate constant k_1 was determined by a least-squares curve fit using a Macintosh personal computer. The pseudo-first-order plots of $\ln(A_\infty - A)$ versus time were linear for three or more half-lives with the correlation coefficient $\rho > 0.999$. Second-order rate constants were calculated from the slope of k_1 versus the concentration of excess substrate by the least-squares analysis.

Electrochemical Measurements. Electrochemical measurements were performed on a BAS 100 W electrochemical analyzer in deaerated acetonitrile containing 0.10 M $NBu^n_4ClO_4$ as a supporting electrolyte at 298 K. A conventional three-electrode cell was used with a platinum-working electrode (surface area of 0.3 mm^2), and a platinum wire was used as the counter electrode. The working electrode was polished with BAS polishing alumina suspension and rinsed with acetone before use. The measured potentials were recorded with respect to an $Ag/AgNO_3$ (0.01 M) reference electrode and converted to vs SCE by adding 0.29 V.[32]

(14) (a) Marcus, R. A.; Eyring, H. *Annu. Rev. Phys. Chem.* **1964**, *15*, 155. (b) Marcus, R. A.; Sutin, N. *Biochim. Biophys. Acta* **1985**, *811*, 265.
(15) Rorabacher, D. B. *Chem. Rev.* **2004**, *104*, 651.
(16) (a) Hathaway, B. J.; Billing, D. E. *Coord. Chem. Rev.* **1970**, *5*, 143. (b) Hathaway, B. J. *Coord. Chem. Rev.* **1981**, *35*, 211.
(17) Guss, J. M.; Bartunik, H. D.; Freeman, H. C. *Acta Crystallogr*. **1992**, *B48*, 790.
(18) Adman, E. T. *Adv. Protein Chem.* **1991**, *42*, 145−197.
(19) (a) Solomon, E. I.; Lowery, M. D. *Science* **1993**, *259*, 1575. (b) Randall, D. W.; Gamelin, D. R.; LaCroix, L. B.; Solomon, E. I. *J. Biol. Inorg. Chem.* **2000**, *5*, 16. (c) Penfield, K. W.; Gewirth, A. A.; Solomon, E. I. *J. Am. Chem. Soc.* **1985**, *107*, 4519.
(20) (a) Solomon, E. I.; Baldwin, M. J.; Lowery, M. D. *Chem. Rev.* **1992**, *92*, 521. (b) Solomon, E. I.; Szilagyi, R. K.; George, S. D.; Basumallick, L. *Chem. Rev.* **2004**, *104*, 419.
(21) (a) Kitajima, N.; Fujisawa, K.; Moro-oka, Y. *J. Am. Chem. Soc.* **1990**, *112*, 3210. (b) Kitajima, N.; Fujisawa, K.; Tanaka, M.; Moro-oka, Y. *J. Am. Chem. Soc.* **1992**, *114*, 9232.
(22) (a) Holland, P. L.; Tolman, W. B. *J. Am. Chem. Soc.* **1999**, *121*, 7270. (b) Holland, P. L.; Tolman, W. B. *J. Am. Chem. Soc.* **2000**, *122*, 6331.
(23) (a) Randall, D. W.; DeBeer George, S.; Holland, P. L.; Hedman, B.; Hodgson, K. O.; Tolman, W. B.; Solomon, E. I. *J. Am. Chem. Soc.* **2000**, *122*, 11632. (b) Randall, D. W.; DeBeer George, S.; Hedman, B.; Hodgson, K. O.; Fujisawa, K.; Solomon, E. I. *J. Am. Chem. Soc.* **2000**, *122*, 11620.
(24) (a) Anderson, O. P.; Perkins, C. M.; Brito, K. K. *Inorg. Chem.* **1983**, *22*, 1267. (b) Sugiura, Y. *Inorg. Chem.* **1978**, *17*, 2176.
(25) Kim, Y.-J.; Kim, S.-O.; Kim, T.-I.; Choi, S.-N. *Inorg. Chem.* **2001**, *40*, 4481.
(26) Hoffmann, S. K.; Corvan, P. J.; Singh, P.; Sethulekshmi, C. N.; Metzger, R. M.; Hatfield, W. E. *J. Am. Chem. Soc.* **1983**, *105*, 4608.
(27) Pawlowski, V.; Kunkely, H.; Zabel, M.; Vogler, A. *Inorg. Chim. Acta* **2004**, *357*, 824.
(28) Liu, S.-J.; Huang, C.-H.; Chang, C.-C. *Mater. Chem. Phys.* **2003**, *82*, 551.
(29) Tran, D.; Skelton, B. W.; White, A. H.; Laverman, L. E.; Ford, P. C. *Inorg. Chem.* **1998**, *37*, 2505.
(30) Although [Cu(SP)(mmt)] has a relatively large extinction coefficient at 736 nm ($\epsilon = 2000\ M^{-1}\ cm^{-1}$) due to the S → Cu^{II} charge transfer (CT) band,[25] $[Cu(dmp)_2]^{2+}$ has a much smaller extinction coefficient at 740 nm ($\epsilon = 100\ M^{-1}\ cm^{-1}$), see: Sundararajan, S.; Wehry, E. L. *J. Phys. Chem.* **1972**, *76*, 1528.
(31) Nazeeruddin, M. K.; Zakeeruddin, S. M.; Humphry-Baker, R.; Liska, J. P.; Shklover, N. V.; Fischer, C.-H.; Grätzel, M. *Inorg. Chem.* **1999**, *38*, 6298.

Preparation of Working Electrodes for Dye-Sensitized Solar Cells. Nanoporous TiO_2 electrode consisted of a TiO_2 film with a triple-layer structure. A compact blocking underlayer of coated TiO_2 was deposited onto an optically transparent electrode (OTE) (Nippon Sheet Glass, SnO_2:F, 8 Ω/cm^2). A solution of titanium tetraisopropoxide in an ethanol−water mixed solution was spin-coated on the OTE surface. The resulting electrodes were annealed at 450 °C in air for 30 min. A transparent layer was prepared by dropping and spreading the colloidal suspensions of TiO_2 nanoparticles (P25, $d = 21$ nm, Nippon Aerogel) on OTE with a glass rod and adhesive tapes as a spacer. The resulting electrodes (OTE/TiO_2) were annealed at 450 °C in air for 30 min. The thickness of the electrodes ranged between 4 and 5 μm as measured by a profiler. Post-treatment with an aqueous solution of $TiCl_4$ was then carried out according to a previously published procedure.[6] A scattering layer was prepared by using TiO_2 nanoparticles ($d = 400$ nm, Nippon Shokubai) under the same experimental conditions as described above.

Coloration of the TiO_2 surface with the Ru dye (N719)[30] was carried out by immersing the film (still warm, i.e., 80−100 °C) for 12 h in a *tert*-butyl alcohol−acetonitrile (1:1) mixture containing 3.0×10^{-4} M of N719. After completion of the dye adsorption, the electrode was withdrawn from the solution, washed with acetonitrile, and dried.

Electrolyte solutions were prepared by dissolving a copper complex redox mediator (0.2 M, $Cu^{II}/(Cu^{I}+Cu^{II}) = 0.4$), *tert*-butylpyridine (0.5 M), and $LiClO_4$ (0.5 M) in anhydrous methoxyacetonitrile.

Photoelectrochemical Measurements. Photocurrent−voltage characteristics of solar cells were measured using a voltage−current source monitor (Advantest R6246) under AM 1.5 simulated light source (Yamashita Denso, YSS-80). Measurements of incident photon-to-photocurrent efficiency (IPCE) were carried out using a setup for IPCE measurements (PV-25DYE, JASCO) under 5 mW/cm^2 monochromatic light illuminations. Solar cells were made by placing the Pt sputtered optically transparent electrode (F-doped SnO_2 sheet resistance 10 Ω/cm^2, Asahi Glass) on the dye-coated TiO_2 film. The electrolyte was injected from one hole made on the counter electrode. The gap between the porous dye coated-TiO_2 electrode and the Pt sputtered-counter electrode was adjusted to be a few tens micrometers and sealed using thermal adhesive films (HIMILAN 1652: Mitsui-Dupont Polychemical), and the electrodes were sealed by heat. The injection holes were sealed by cover glass (Iwaki Glass), HIMILAN film, and epoxy resin (Torr seal: Varian Vacuum Products).

Results and Discussion

Kinetics of Electron Transfer from Ferrocene Derivatives to Copper Complexes. To compare the electron-transfer reactivities of all of the copper complexes employed in this study, the kinetic studies on the reduction of copper complexes by ferrocene derivatives were performed. The one-electron reduction potentials (E^0_{red} vs SCE) of [Cu(SP)(mmt)], [Cu(dmp)$_2$](CF$_3$SO$_3$)$_2$, and [Cu(phen)$_2$](CF$_3$SO$_3$)$_2$ in acetonitrile (MeCN) were determined to be 0.29, 0.66, and −0.10 V, respectively (see Supporting Information S1). Thus, ferrocene derivatives with less positive oxidation potentials than the E^0_{red} values of copper complexes were chosen as reductants to examine the kinetics of the electron transfer from ferrocene derivatives to copper complexes: [Fe(C$_5$H$_4$Me)$_2$] ($E^0_{red} = 0.26$ V),[33] [Fe(C$_5$H$_5$)(C$_5$H$_4$COOBz)] ($E^0_{red} = 0.57$ V), and [Fe(C$_5$Me$_5$)$_2$] ($E^0_{red} = -0.08$ V)[33] for the electron-transfer reduction of [Cu(SP)(mmt)], [Cu(dmp)$_2$](CF$_3$SO$_3$)$_2$, and [Cu(phen)$_2$]−(CF$_3$SO$_3$)$_2$, respectively.

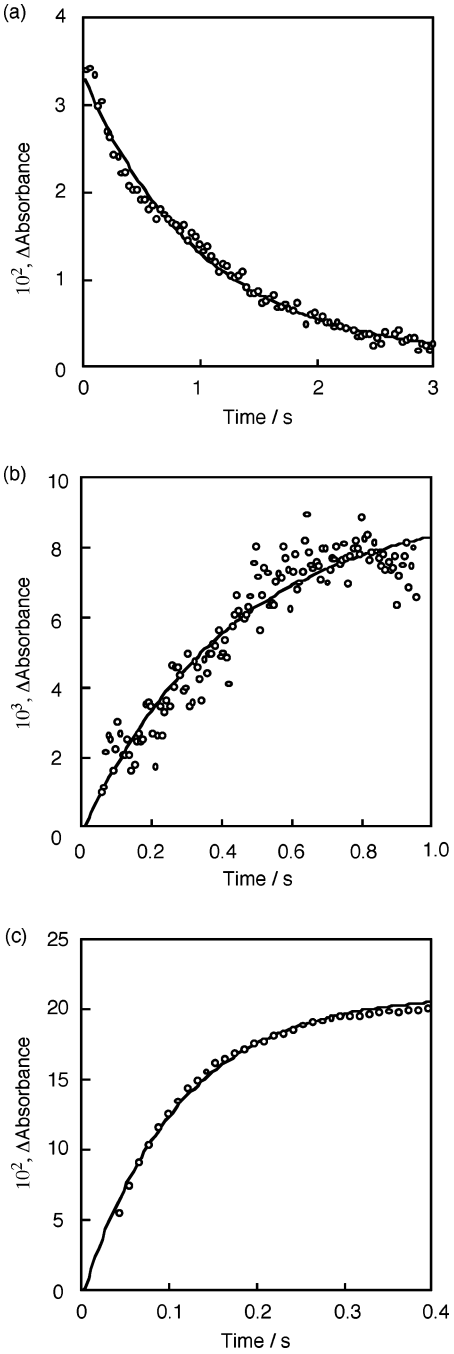

Figure 2. Kinetic curves for reduction of (a) [Cu(SP)(mmt)] (3.0×10^{-5} M) by [Fe(C$_5$H$_4$Me)$_2$] (6.0×10^{-4} M) monitored by a decrease in absorbance at 738 nm due to [Cu(SP)(mmt)], (b) reduction of [Cu(dmp)$_2$](CF$_3$SO$_3$)$_2$ (1.25×10^{-6} M) by [Fe(C$_5$H$_5$)(C$_5$H$_4$COOBzl)] (2.5×10^{-5} M) monitored by an increase in absorbance at 456 nm due to [Cu(dmp)$_2$]$^+$, and (c) reduction of [Cu(phen)$_2$](CF$_3$SO$_3$)$_2$ (5.0×10^{-5} M) by [Fe(C$_5$Me$_5$)$_2$] (1.0×10^{-3} M) monitored by an increase in absorbance at 438 nm due to [Cu(phen)$_2$]$^+$ in MeCN at 298 K.

As shown in Figure 2, the reduction of [Cu(SP)(mmt)], [Cu(dmp)$_2$](CF$_3$SO$_3$)$_2$, and [Cu(phen)$_2$](CF$_3$SO$_3$)$_2$ was detected by monitoring a decrease in the Cu^{II} absorption band at 738 nm, an increase in the Cu^{I} absorption band at 456 nm, and an increase in the Cu^{I} absorption band at 438 nm, respectively.[25,34,35] The rates obeyed pseudo-first-order kinetics under the present experimental conditions where concentrations of

(32) Mann, C. K.; Barnes, K. K. *Electrochemical Reactions in Nonaqueous Systems*; Marcel Dekker: New York, 1970.
(33) (a) Fukuzumi, S.; Mochizuki, S.; Tanaka, T. *Inorg. Chem.* **1989**, *28*, 2459. (b) Fukuzumi, S.; Okamoto, K.; Gros, C. P.; Guilard, R. *J. Am. Chem. Soc.* **2004**, *126*, 10441.
(34) Doine, H.; Yano, Y.; Swaddle, T. W. *Inorg. Chem.* **1989**, *28*, 2319.

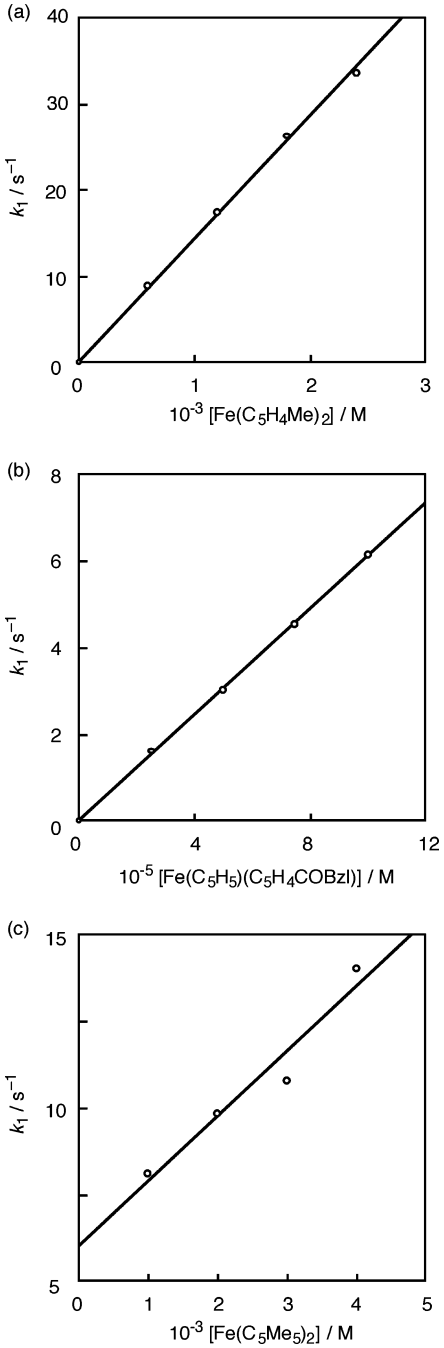

Figure 3. Plot of pseudo-first-order rate constants k_1 versus concentrations of (a) [Fe(C_5H_4Me)$_2$] for the reduction of [Cu(SP)(mmt)], (b) [Fe(C_5H_5)($C_5H_4COOBzl$)] for the reduction of [Cu(dmp)$_2$](CF_3SO_3)$_2$, and (c) [Fe(C_5Me_5)$_2$] for the reduction of [Cu(phen)$_2$](CF_3SO_3)$_2$ in MeCN at 298 K.

ferrocene derivatives were greater than a 20-fold excess of the copper complex. The pseudo-first-order rate constants (k_1) increase linearly with increasing concentrations of ferrocene derivatives (Figure 3a−c). Thus, there is no "gated" behavior that exhibits limiting first-order rate, independent of the reductant concentration due to the conformational "gating".[15,36] In the case of electron transfer from Fe(C_5Me_5)$_2$] (−0.08 V vs SCE)[33] to [Cu(phen)$_2$](CF_3SO_3)$_2$ (−0.10 V vs SCE), the free energy change of electron transfer is slightly positive (ΔG_{et}^0 = +0.02 eV), when the electron-transfer reaction is reversible (in equilibrium) at 298 K. In such a case, k_1 is expressed by eq 1,

$$k_1 = k_{21} + k_{12}[\mathrm{Fc}] \quad (1)$$

where k_{12} and k_{21} are the forward and back electron-transfer rate constants, respectively.

From the slope and intercept were determined the k_{12} and k_{21} values, from which the electron-transfer equilibrium constant K (=k_{12}/k_{21}) was obtained as 310 M^{-1}. This value agrees with the K value (320 M^{-1}) determined independently from the spectral titration (see Supporting Information S2). The k_{12} values are obtained from the slope of the plots. The k_{12} values of [Cu(SP)(mmt)], [Cu(dmp)$_2$](CF_3SO_3)$_2$, and [Cu(phen)$_2$](CF_3SO_3)$_2$ are listed in Table 1.

Table 1. Electron Self-Exchange Rate Constants (k_{22}) of Copper Complexes

copper complex	ferrocene derivative	$\Delta G_{et}^{0\,a}$ (eV)	$10^{-4}k_{12}{}^b$ (M^{-1} s^{-1})	k_{22} (M^{-1} s^{-1})
[Cu(SP)(mmt)]	[Fe(C_5H_4Me)$_2$]	−0.03	1.4	7.7
[Cu(dmp)$_2$](CF_3SO_3)$_2$	[Fe(C_5H_5)($C_5H_4COOBzl$)]	−0.09	6.1	23
[Cu(phen)$_2$](CF_3SO_3)$_2$	[Fe(C_5Me_5)$_2$]	0.02	0.19	0.20

[a] Free energy change of electron transfer from ferrocene derivatives to copper(II) complexes. [b] Rate constants (k_{12}) of electron transfer from ferrocene derivatives to copper complexes.

Electron Self-Exchange Rate Constants of Copper Complexes. The electron self-exchange rate constants of [Cu(phen)$_2$](CF_3SO_3)$_2$ and [Cu(dmp)$_2$](CF_3SO_3)$_2$ have been reported previously.[34,37] However, the self-exchange rate constants of copper complexes determined by NMR analyses were sensitively influenced by their experimental conditions, and there has been controversy on the self-exchange rate constants of copper complexes.[15] Here, we compare the electron-transfer reactivities of copper complexes under the same experimental conditions using a homologous series of ferrocene derivatives. Ferrocene derivatives are known to react by an outer-sphere mechanism in a variety of electron-transfer processes especially with inorganic oxidants.[38] A quantitative discussion on electron-transfer characteristics of copper complexes can be achieved by comparing the observed rates of outer-sphere electron transfer to those predicted by the Marcus theory for the rates of outer-sphere electron-transfer reactions.[14,15] The Marcus relation for the rate constant of the electron transfer from the reductant to the oxidant, k_{12}, is given by eq 2,[14]

$$k_{12} = (k_{11}k_{22}K_{12}f)^{1/2} \quad (2)$$

where k_{11} and k_{22} are the rate constants of the corresponding self-exchanges, and K_{12} is the equilibrium constant for the electron-transfer reaction. The K_{12} value is obtained from the oxidation potential of the reductant, E_{ox}^0, and the reduction potential of the oxidant, E_{red}^0, by using eq 3.[14,39] The parameter f in eq 2 is given by eq 4, in which the frequency factor Z is taken as 1×10^{11} M^{-1} s^{-1}.[14] The reported values of self-

$$\log K_{12} = [F/(-2.3RT)](E_{ox}{}^0 - E_{red}{}^0) \quad (3)$$

$$\log f = (\log K_{12})^2/[4\log(k_{11}k_{22}/Z^2)] \quad (4)$$

exchange rate constants (k_{11}) for [Fe(C_5H_4Me)$_2$] (8.3×10^6 M^{-1} s^{-1}) and [Fe(C_5Me_5)$_2$] (3.8×10^7 M^{-1} s^{-1}) constitute a

(35) Goldstein, S.; Czapski, G. *J. Am. Chem. Soc.* **1983**, *105*, 7276.
(36) Koshino, N.; Kuchiyama, Y.; Funahashi, S.; Takagi, H. D. *Chem. Phys. Lett.* **1999**, *306*, 291.

satisfactory basis for accounting for the experimental kinetic data when considered in light of the Marcus relation (eqs 2−4).[39] The electron self-exchange rate constant (k_{11}) of [Fe(C_5H_5)(C_5H_4-COOBzl)] was taken as that of [Fe(C_5H_5)$_2$] (5.3×10^6 M^{-1} s^{-1}).[40] The reduction of [Cu(SP)(mmt)] by [Fe($C_5H_4Bu^n$)$_2$] ($k_{11} = 4.9 \times 10^6$ M^{-1} s^{-1}) was also examined to determine the k_{22} value for the electron self-exchange between [Cu(SP)(mmt)] and [Cu(SP)(mmt)]$^-$ (see Supporting Information S3). The k_{22} value of [Cu(SP)(mmt)]/[Cu(SP)(mmt)]$^-$ determined from electron transfer from [Fe(C_5H_4Me)$_2$] to [Cu(SP)(mmt)] (7.7 M^{-1} s^{-1}) agrees with that determined independently from electron transfer from [Fe($C_5H_4Bu^n$)$_2$] to [Cu(SP)(mmt)] (10.7 M^{-1} s^{-1}). Such an agreement demonstrates that the electron transfer between copper complexes and ferrocene derivatives proceeds by an outer-sphere mechanism.

Table 1 lists all of the k_{22} values of copper complexes determined in this study. The self-exchange rate constant of a blue copper model complex, [Cu(SP)](mmt)], is 40 times larger than that of a reference copper complex, [Cu(phen)$_2$](CF_3SO_3)$_2$. The k_{22} of [Cu(dmp)$_2$](CF_3SO_3)$_2$ is even larger, and it is 100 times larger than that of [Cu(phen)$_2$](CF_3SO_3)$_2$. This indicates that S ligands of blue copper are not essential to attain the efficient electron-transfer properties of copper complexes. The order of k_{22} found in this study is well reflected as the difference in geometries between copper(I) and copper(II) (vide infra). The X-ray crystal structures of [Cu(SP)](mmt)] and [Cu(dmp)$_2$]$^{2+/+}$ have been reported previously.[25,27,41] The Cu^{II} atom of [Cu(SP)](mmt)] adopts a distorted tetragonal geometry with a dihedral angle of 68° between the N_2Cu and the S_2Cu planes.[25] The Cu^{I} atom of [Cu(SP)(mmt)]$^-$ may adopt a normal tetrahedral geometry. On the other hand, both Cu^{II} and Cu^{I} atoms of [Cu(dmp)$_2$]$^{2+/+}$ adopt distorted tetragonal geometries with dihedral angles of 70° and 78°, respectively.[27,41] Thus, the coordination geometry change between Cu^{II} and Cu^{I} of [Cu(dmp)$_2$]$^{2+/+}$ is certainly smaller than that of [Cu(SP)(mmt)]$^{0/-}$, leading to the larger k_{22} value for [Cu(dmp)$_2$]$^{2+/+}$ than that for [Cu(SP)(mmt)]$^{0/-}$.

DSSCs Using Copper Complexes as Redox Couples. The electrolyte solutions were prepared by dissolving 0.2 M copper complex, 0.5 M *tert*-butylpyridine, and 0.5 M $LiClO_4$ in methoxyacetonitrile. The Cu^{II}/(Cu^{I}+Cu^{II}) ratio was varied to determine the optimized ratio as 0.4 (Cu^{I} of 0.12 M and Cu^{II} of 0.08 M, see Supporting Information S4). We used TiO_2 films having a triple-layered structure, in which the first layer is a compact blocking underlayer, the second a transparent layer (P25), and the third a scattering layer as in the case of Grätzel's report.[6b] The compact blocking layer and scattering layer have a better effect on photocurrent generation, respectively (Supporting Information S5, S6). In addition, the film thickness of the transparent layer was optimized as 4−5 μm because the photochemical measurements of DSSCs consist of some thickness (Supporting Information S7).

A series of photocurrent action spectra were recorded to evaluate the photoelectrochemical response of DSSCs using copper complexes. The monochromatic incident photon-to-photocurrent conversion efficiency (IPCE), defined as the number of electrons generated by light in the outer circuit divided by the number of incident photons, was determined by using eq 5,[42]

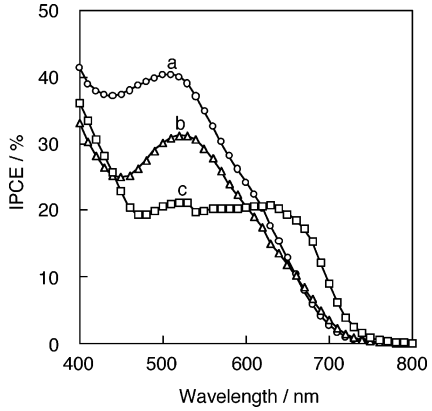

Figure 4. Comparison of photocurrent action spectra (IPCE values) of DSSCs containing (a) [Cu(SP)(mmt)]$^{0/-}$, (b) [Cu(dmp)$_2$]$^{2+/+}$, and (c) [Cu(phen)$_2$]$^{2+/+}$ as the redox couples.

$$\text{IPCE (\%)} = 100 \times 1240 \times I_{sc}(\text{mA/cm}^2)/[\lambda(\text{nm}) \times P_{in}(\text{mW/cm}^2)] \quad (5)$$

where I_{sc} is the short circuit photocurrent generated by monochromatic light, λ is the wavelength of incident monochromatic light, and whose light intensity is P_{in}.

Figure 4 shows the photocurrent action spectra of DSSCs using [Cu(SP)(mmt)]$^{0/-}$, [Cu(dmp)$_2$]$^{2+/+}$, and [Cu(phen)$_2$]$^{2+/+}$. The IPCE values of DSSCs increase in order: DSSC using [Cu(phen)$_2$]$^{2+/+}$ < [Cu(dmp)$_2$]$^{2+/+}$ < [Cu(SP)(mmt)]$^{0/-}$. The maximum of IPCE value reaches 40% in the case of the DSSC using [Cu(SP)(mmt)]$^{0/-}$.

The current−voltage (I−V) characteristics of DSSCs using copper complexes were examined using a thin-layer sandwich-type solar cell under illumination of simulated AM 1.5 solar light (100 mW/cm^2 from a Xe lamp) to determine the light energy conversion efficiency (η). The dye-coated TiO_2 film as a working electrode was placed directly on top of an OTE as a counter electrode, on which the Pt was sputtered. The redox electrolyte containing a copper complex was injected from a hole made on the counter electrode to the inter-electrode space. The solar cells were illuminated in the front through a conducting glass substrate. Light energy conversion efficiency, η, is calculated by eq 6,[43]

$$\eta = FF \times I_{sc} \times V_{oc}/P_{in} \quad (6)$$

where the fill factor (FF) is defined as $FF = [IV]_{max}/I_{sc}V_{oc}$, where V_{oc} is the open-circuit photovoltage, and I_{sc} is the short circuit photocurrent.

(37) Lee, C.-W.; Anson, F. C. *Inorg. Chem.* **1984**, *23*, 837.
(38) (a) Pladziewicz, J. R.; Espenson, J. H. *J. Am. Chem. Soc.* **1973**, *95*, 56. (b) Pelizzetti, E. *Inorg. Chem.* **1979**, *18*, 1386. (c) Borchardt, D.; Pool, K.; Wherland, S. *Inorg. Chem.* **1982**, *21*, 93. (d) Borchardt, D.; Wherland, S. *Inorg. Chem.* **1986**, *25*, 901.
(39) The work terms are neglected, because in the present case one of the reactants and products is uncharged.
(40) Yang, E. S.; Chan, M.-S.; Wahl, A. C. *J. Phys. Chem.* **1980**, *84*, 3094.
(41) Tran, D.; Skelton, B. W.; White, A. H.; Laverman, L. E.; Ford, P. C. *Inorg. Chem.* **1998**, *37*, 2505.
(42) Khazraji, A. C.; Hotchandani, S.; Das, S.; Kamat P. V. *J. Phys. Chem. B* **1999**, *103*, 4693.
(43) (a) Kamat, P. V.; Barazzouk, S.; Thomas, K. G.; Hotchandani, S. *J. Phys. Chem. B* **2000**, *104*, 4014. (b) Sudeep P. K.; Ipe, B. I.; Thomas, K. G.; George, M. V.; Barazzouk, S.; Hotchandani, S.; Kamat, P. V. *Nano Lett.* **2002**, *2*, 29. (c) Kamat, P. V.; Barazzouk, S.; Hotchandani, S.; Thomas, K. G. *Chem.-Eur. J.* **2000**, *6*, 3914.

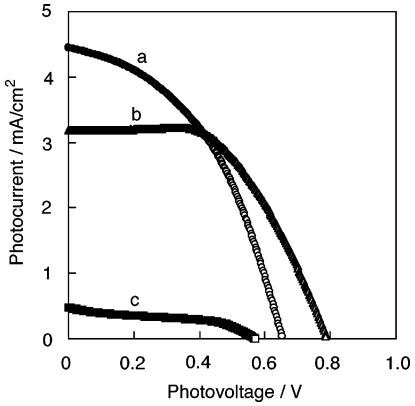

Figure 5. Photocurrent−photovoltage curves of DSSCs containing (a) $[Cu(SP)(mmt)]^{0/-}$, (b) $[Cu(dmp)_2]^{2+/+}$, and (c) $[Cu(phen)_2]^{2+/+}$ as the redox couples; input power: 100 mW/cm^2.

Table 2. Performance Characteristics of DSSCs Using Various Copper Complexes under White Light Illumination; Input Power: 100 mW/cm^2

redox couple	$[Cu(SP)(mmt)]^{0/-}$	$[Cu(dmp)_2]^{2+/+}$	$[Cu(phen)_2]^{2+/+}$
I_{sc}/mA/cm^2	4.4	3.2	0.48
V_{oc}/V	0.66	0.79	0.57
FF	0.44	0.55	0.43
η/%	1.3	1.4	0.12

Figure 5 shows the I−V characteristics of DSSCs using copper complexes. The short circuit photocurrents (I_{sc}), open-circuit photovoltages (V_{oc}), and fill factors (*FF*) are summarized in Table 2 together with the light energy conversion efficiencies (η), which are determined using eq 6. The V_{oc} values of copper complexes increase in the order: $[Cu(phen)_2]^{2+/+}$ (0.57 V), $[Cu(SP)(mmt)]^{0/-}$ (0.66 V), and $[Cu(dmp)_2]^{2+/+}$ (0.79 V), in agreement with the order of the redox potentials of copper complexes. The η values of DSSCs using $[Cu(phen)_2]^{2+/+}$, $[Cu(dmp)_2]^{2+/+}$, and $[Cu(SP)(mmt)]^{0/-}$ were determined as 0.1%, 1.4%, and 1.3%, respectively.

The difference in the photochemical properties of DSSCs using different copper complexes may result from both the thermodynamics and the kinetics of electron-transfer processes of $[Cu(SP)(mmt)]^{0/-}$, $[Cu(dmp)_2]^{2+/+}$, and $[Cu(phen)_2]^{2+/+}$ in the photocurrent generation in DSSCs (vide infra). First, the excited state of N719 dye injects an electron to the conduction band of TiO_2 to produce the dye cation. The resulting N719 dye cation is reduced by the Cu^I complex to form the Cu^{II} complex, which is reduced at the Pt counter electrode, leading to the photocurrent generation. The worst photovoltaic properties with the $[Cu(phen)_2]^{2+/+}$ mediator (the lowest I_{sc} and V_{oc}) certainly result from the slowest electron self-exchange rate of $[Cu(phen)_2]^{2+/+}$ and the lowest redox potential (−0.10 V vs SCE). Both the I_{sc} and the V_{oc} values are improved in DSSC with $[Cu(SP)(mmt)]^{0/-}$ because of the much faster electron self-exchange rate of $[Cu(SP)(mmt)]^{0/-}$ and the higher redox potential (0.29 V). In the case of $[Cu(dmp)_2]^{2+/+}$, the I_{sc} value is smaller than the case of $[Cu(SP)(mmt)]^{0/-}$ despite the faster electron self-exchange rate than that of $[Cu(SP)(mmt)]^{0/-}$, probably because of the significantly smaller driving force of electron transfer from $[Cu(dmp)_2]^{2+/+}$ to the dye cation as compared to $[Cu(SP)(mmt)]^{0/-}$. However, this drawback is compensated by the higher V_{oc} value due to the higher redox potential (0.66 V) of $[Cu(dmp)_2]^{2+/+}$ than that of $[Cu(SP)(mmt)]^{0/-}$. Thus, the potential mismatch between the redox couples of the sensitizers (S^+/S) and the mediator is least for the $[Cu(dmp)_2]^{2+/+}$.

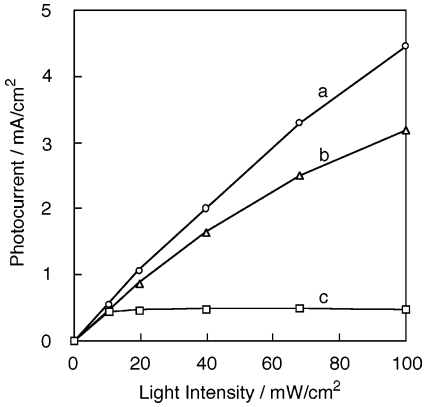

Figure 6. Relationship between light intensity and short circuit photocurrents of DSSCs containing (a) $[Cu(SP)(mmt)]^{0/-}$, (b) $[Cu(dmp)_2]^{2+/+}$, and (c) $[Cu(phen)_2]^{2+/+}$ as the redox couples.

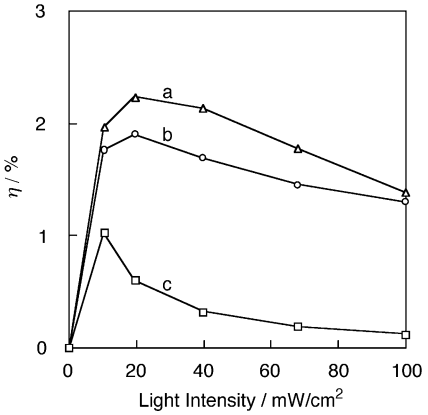

Figure 7. Relationship between light intensity and energy conversion efficiencies of DSSCs containing (a) $[Cu(SP)(mmt)]^{0/-}$, (b) $[Cu(dmp)_2]^{2+/+}$, and (c) $[Cu(phen)_2]^{2+/+}$ as the redox couples.

The photovoltaic measurements were also performed under the irradiation of various power lights. Figure 6 shows some I_{sc} values for various input light powers. The I_{sc} values of DSSCs using $[Cu(SP)(mmt)]^{0/-}$ and $[Cu(dmp)_2]^{2+/+}$ increase as the input light power increases. In contrast, the I_{sc} value of DSSC using $[Cu(phen)_2]^{2+/+}$ reaches a constant value under the same experimental conditions. This indicates that the back electron transfer from TiO_2 to the dye cation becomes faster than the electron transfer from $[Cu(phen)_2]^+$ to the dye cation at the high light power region above 10 mW/cm^2 because of the slow electron transfer from $[Cu(phen)_2]^+$.

The dependence of the η values on the input light power is shown in Figure 7. The maximum η value (2.3%) is attained for DSSC using $[Cu(dmp)_2]^{2+/+}$ under light irradiation of 20 mW/cm^2 intensity. The photoelectrochemical responses of DSSCs with $[Cu(SP)(mmt)]^{0/-}$ and $[Cu(dmp)_2]^{2+/+}$ redox couples are compared to the corresponding DSSC with the I_3^-/I^- redox couple. The IPCE values at 510 nm of DSSCs using $[Cu(SP)(mmt)]^{0/-}$, $[Cu(dmp)_2]^{2+/+}$, and I_3^-/I^- as redox couples are obtained as 40%, 31%, 60%, respectively (see Supporting Information S8). The light energy conversion efficiencies of DSSCs using $[Cu(SP)(mmt)]^{0/-}$, $[Cu(dmp)_2]^{2+/+}$, and I_3^-/I^- as redox couples are determined as 1.9%, 2.2%, and 4.3% under

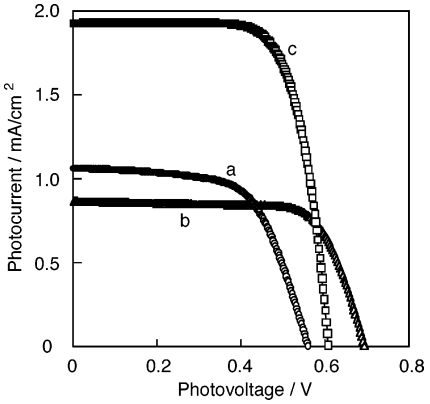

Figure 8. I−V curves of DSSCs using (a) $[Cu(SP)(mmt)]^{0/-}$, (b) $[Cu(dmp)_2]^{2+/+}$, and (c) I_3^-/I^- as the redox couples; input power: 20 mW/cm^2. I_3^-/I^-: 0.2 M LiI, 0.05 M I_2, 0.3 M 1,2-dimethyl-3-propylimidazolium iodide, and 0.5 M *tert*-butylpyridine in methoxyacetonitrile.

weak illumination of simulated AM 1.5 solar light (20 mW/cm^2, from a Xe lamp), respectively (Figure 8).

Conclusions

We have evaluated the electron self-exchange rate constants of $[Cu(SP)(mmt)]^{0/-}$, $[Cu(dmp)_2]^{2+/+}$, and $[Cu(phen)_2]^{2+/+}$ based on electron-transfer reactions from a homologous series of ferrocene derivatives to the copper(II) complexes in light of the Marcus theory of electron transfer. The resulting electron self-exchange rate constant (k_{22}) increases in the order: $[Cu(phen)_2]^{2+/+} < [Cu(SP)(mmt)]^{0/-} < [Cu(dmp)_2]^{2+/+}$, in agreement with the order of the smaller structural change between the copper(II) and copper(I) complexes. We then have constructed the dye-sensitized solar cells (DSSC) using the copper complexes as redox couples to compare the photoelectrochemical responses with those using the conventional I_3^-/I^- couple. The maximum η value was attained as 2.2% for DSSC using $[Cu(dmp)_2]^{2+/+}$ under the weak solar light irradiation of 20 mW/cm^2 intensity. Although the light energy conversion efficiency of DSSCs using blue copper model complexes with a distorted tetragonal geometry as the redox couples is still lower than that of the conventional I_3^-/I^- couple, the higher V_{oc} value is attained for the DSSC with $[Cu(dmp)_2]^{2+/+}$ for the first time as compared to that using the I_3^-/I^- couple. This is particularly important because the dmp ligand is commercially available and $[Cu(dmp)_2]^{2+/+}$ complexes are readily made in one step. The use of copper model complexes with a distorted tetragonal geometry, in which the structural change between the copper(I) and copper(II) complexes is minimized, provides a promising strategy to develop efficient and low cost photovoltaic cells, because nature has successfully utilized such a strategy to develop efficient electron-transport systems using blue copper protein as electron mediators.

Acknowledgment. This work was partially supported by a Grant-in-Aid (No. 16205020) from the Ministry of Education, Culture, Sports, Science, and Technology, Japan. We are grateful to Dr. Takayuki Kitamura, Osaka University, for helping with the preparation of DSSC.

Supporting Information Available: Cyclic voltammograms of copper complexes (S1), the titration of $[Cu(phen)_2](CF_3SO_3)_2$ by excess $[Fe(C_5Me_5)_2]$ (S2), plot of pseudo-first-order rate constants k_1 versus $[Fe(C_5H_4{}^nBu)_2]$ concentration for the reduction of [Cu(SP)(mmt)] (S3), plot of η value versus Cu^{II}/Cu^{I} concentrations ratio of DSSC using [Cu(SP)(mmt)] (S4), I−V curves of DSSCs using [Cu(SP)(mmt)] with and without compact blocking layer (S5), I−V curves of DSSCs using [Cu(SP)(mmt)] with and without scattering layer (S6), plot of η value versus transparent layer film thickness (S7), and photocurrent action spectra (IPCE values vs wavelength) with input power: 20 mW/cm^2 (S8). This material is available free of charge via the Internet at http://pubs.acs.org.

JA0506814